Supplementary Materials: Urban Growth Dynamics in Perth, Western Australia: Using Applied Remote Sensing for Sustainable Future Planning

Andrew MacLachlan, Eloise Biggs, Gareth Roberts and Bryan Boruff

This supplementary material supports the main text as follows:

Materials and Methods

S1. Standardisation and Normalisation

The non-urban land cover class was composed of four classes defined based on existing literature (e.g., [1–3]) and study area characteristics. These classes were forest, water, grassland and bare earth. Grassland and forest were also merged to create a single vegetation class. A complete set of land cover classes enabled examination of statistical differences generated from normalisation (Figure S1). The Coefficient of Variation (CV) statistic was calculated to describe the amount of variability relative to the mean spectral reflectance of the post classification datasets [4][1]. The CV was calculated for pre- and post-normalisation datasets for both intra-year class reflectance, which describes the variability within each class per year, and the inter-year reflectance, which describes the variability of each class across all imagery dates. Post-normalised Landsat data exhibited statistically significant lower inter- and intra-CV with T = 0, Z = −2.154, p = 0.016, r = −0.359 and T = 0, Z = −2.418, p = 0.008 r = −0.373, respectively. The test statistic (T) was obtained from dataset differencing (pre- minus post-processed images), representing the lowest value of the sum of positive ranks (values increased) or negative ranks (values decreased). Hence, T = 0 dictates that post-processed data consistently obtained a lower value than pre-processed imagery, statistically significant at $p < 0.05$ [5]. Therefore, reduced intra and inter year variance facilitates more appropriate one model classification for Landsat 5 TM and Landsat 7 ETM+ and another for Landsat 8 OLI.

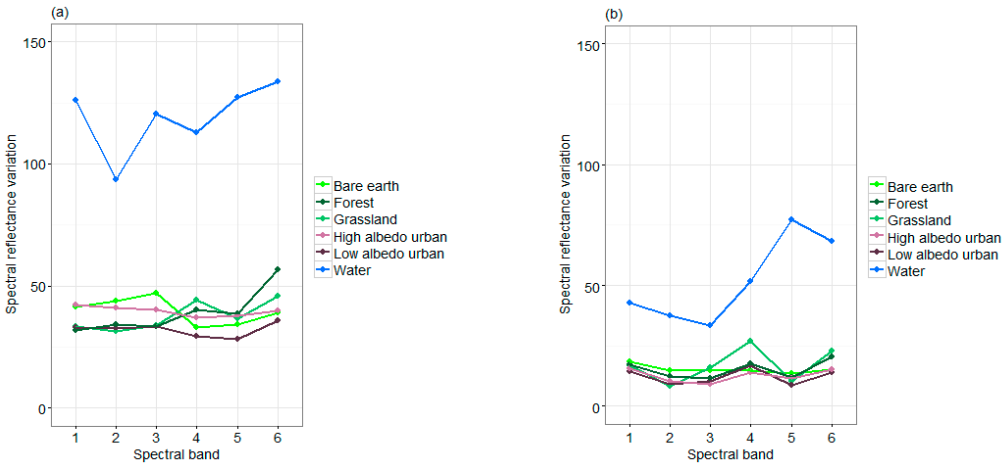

Figure S1. Inter year classification reflectance variation categorised by classified output for each spectral band for: pre (**a**) and post (**b**) normalisation correction.

S2. Accuracy Assessment

For each land use category, 50 random pixels per class per year were visually identified and classified based on the majority land cover within the coincident Landsat pixel from Google Earth

[1] Using R version 3.3.0

imagery for the available years: 2000, 2003, 2005, 2007, 2013 and 2015 [6]. Both user's accuracy (fraction of correctly classified pixels relative to all others classified as a particular land cover), producer's accuracy (fraction of correctly classified pixels compared to ground truth data) and associated Kappa coefficients were consistently high except for the producer accuracy of bare earth which has an average accuracy of 53.33% (Tables S1 and S2). This is due to the known spectral similarities between bare earth and impervious surfaces, and water and shadow which resulted in spectral confusion during classification [3,7–10].

Table S1. Classification accuracy and associated Kappa Coefficient per year of classified Landsat.

Year	Accuracy (%)	Kappa Coefficient
2000	82	0.75
2003	80	0.72
2005	82	0.74
2007	84	0.78
2013	79	0.70
2015	79	0.70
Average	81	0.73

Table S2. Producer's and User's accuracy per year of classified Landsat imagery.

Producer Accuracy	**Bare Earth**	**Vegetation**	**Urban**	**Water**
2000	56.00	96.00	90.00	66.00
2003	50.00	97.00	85.00	68.00
2005	52.00	98.00	86.00	72.00
2007	48.00	98.00	83.00	94.00
2013	52.00	99.00	81.00	62.00
2015	62.00	99.00	80.00	52.00
Average	53.33	97.83	84.17	69.00
User Accuracy	**Bare Earth**	**Vegetation**	**Urban**	**Water**
2000	84.85	76.80	84.11	94.29
2003	69.44	76.98	83.33	94.44
2005	81.25	78.40	81.13	97.30
2007	68.57	80.33	87.37	97.92
2013	68.42	73.88	83.51	100.00
2015	75.61	73.88	83.33	89.66
Average	74.69	76.71	83.80	95.60

S3. Local Government Areas

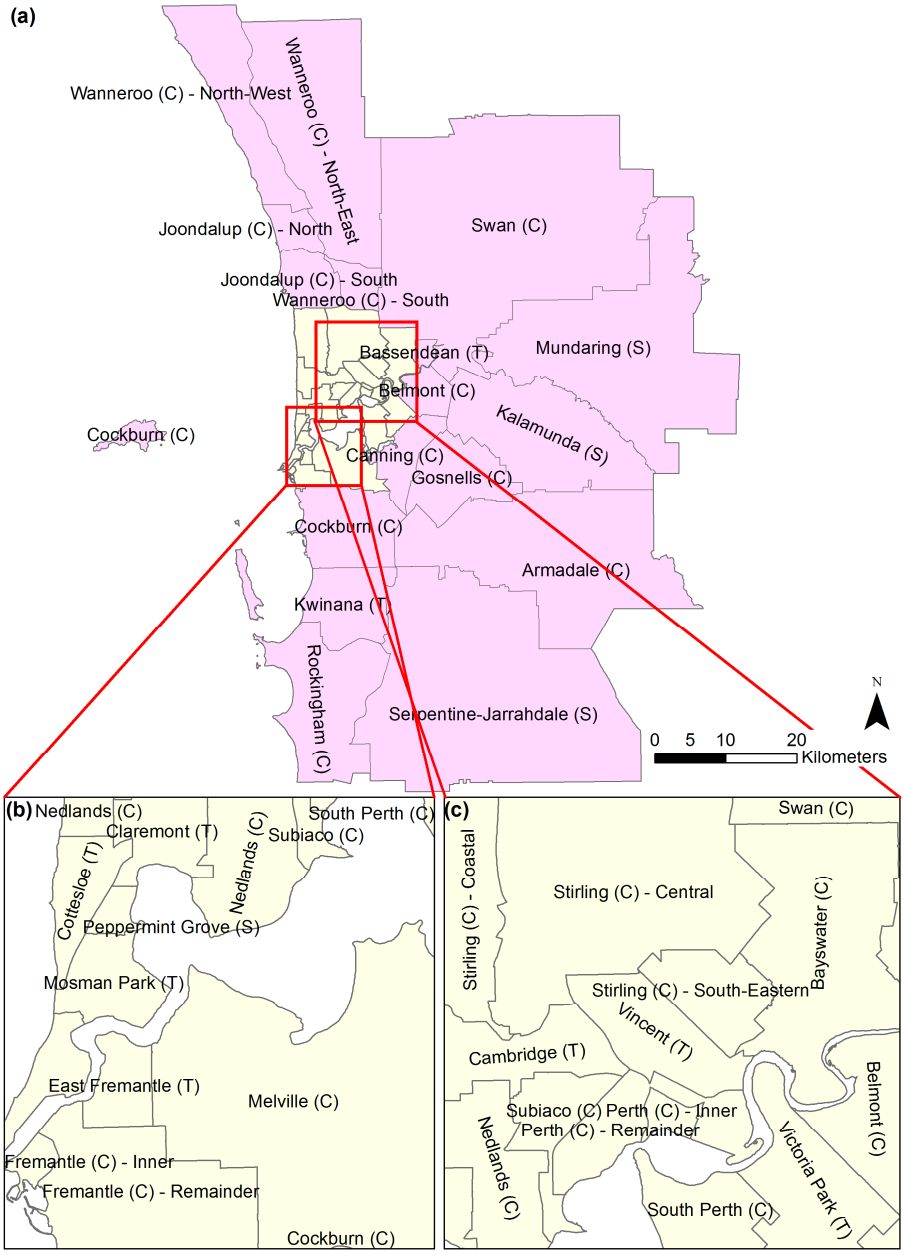

Figure S2. Local Government Areas (LGAs) located in Perth Metropolitan Region (**a**); with (**b**) exhibiting LGAs South and West of the Swan River and (**c**) LGAs North and East of the Swan River.

References

1. Hu, X.; Weng, Q. Estimating impervious surfaces from medium spatial resolution imagery using the self-organizing map and multi-layer perceptron neural networks. *Remote Sens. Environ.* **2009**, *113*, 2089–2102.
2. Schneider, A. Monitoring land cover change in urban and peri-urban areas using dense time stacks of Landsat satellite data and a data mining approach. *Remote Sens. Environ.* **2012**, *124*, 689–704.
3. Feyisa, G.L.; Meilby, H.; Darrel Jenerette, G.; Pauliet, S. Locally optimized separability enhancement indices for urban land cover mapping: Exploring thermal environmental consequences of rapid urbanization in Addis Ababa, Ethiopia. *Remote Sens. Environ.* **2016**, *175*, 14–31.
4. Brown, C.E. *Applied Multivariate Statistics in Geohydrology and Related Sciences*; Springer: Berlin/Heidelberg, Germany, 1998.

5. Field, A. *Discovering Statistics Using SPSS (Introducing Statistical Methods Series)*, 3rd ed.; SAGE Publications Ltd.: London, UK, 2009.
6. Congalton, R.G. Accuracy assessment and validation of remotely sensed and other spatial information. *Int. J. Wildl. Fire* **2001**, *10*, 321–328.
7. Lu, D.; Moran, E.; Hetrick, S. Detection of impervious surface change with multitemporal Landsat images in an urban-rural frontier. *ISPRS J. Photogramm. Remote Sens.* **2011**, *66*, 298–306.
8. Herold, M.; Gardner, M.; Hadley, B.; Roberts, D. The spectral dimension in urban land cover mapping from high-resolution optical remote sensing data. In Proceedings of the 3rd Symposium on remote Sensing of Urban Areas, Istanbul, Turkey, 11–13 June 2002; Volume 6, pp. 1–8.
9. Varshney, A.; Rajesh, E. A Comparative Study of Built-up Index Approaches for Automated Extraction of Built-up Regions From Remote Sensing Data. *J. Indian Soc. Remote Sens.* **2014**, *42*, 659–663.
10. Sawaya, K.E.; Olmanson, L.G.; Heinert, N.J.; Brezonik, P.L.; Bauer, M.E. Extending satellite remote sensing to local scales: Land and water resource monitoring using high-resolution imagery. *Remote Sens. Environ.* **2003**, *88*, 144–156.